ANL-HEP-PR-97-28

Thermodynamics of Lattice QCD with Chiral 4-Fermion Interactions

J. B. Kogut

Department of Physics, University of Illinois, 1110 West Green Street, Urbana, IL 61801, USA

J.-F. Lagaë and D. K. Sinclair

HEP Division, Argonne National Laboratory, 9700 South Cass Avenue, Argonne, IL 60439, USA

Abstract

We have studied lattice QCD with an additional, irrelevant 4-fermion interaction having a $U(1) \times U(1)$ chiral symmetry, at finite temperatures. Adding this 4-fermion term allowed us to work at zero quark mass, which would have otherwise been impossible. The theory with 2 massless staggered quark flavours appears to have a first order finite temperature phase transition at $N_t = 4$ for the value of 4-fermion coupling we have chosen, in contrast to what is expected for 2-flavour QCD. The pion screening mass is seen to vanish below this transition, only to become massive and degenerate with the σ (f_0) above this transition where the chiral symmetry is restored, as is seen by the vanishing of the chiral condensate.

I. INTRODUCTION

Studying the finite temperature phase transition of lattice QCD and the equation of state near this transition requires an understanding of the zero quark mass limit, where molecular dynamics methods fail completely [1,2]. Even at realistic values of the u and d quark masses, the Dirac operator is nearly singular, and iterative methods for its inversion become extremely costly in computer time. [1] For this reason, we modify the lattice QCD action by the addition of an irrelevant, chirally invariant 4-fermion interaction which renders the Dirac operator non-singular, even when the quark mass is zero. Because the extra interaction is irrelevant, such an action should lie in the same universality class as the standard action, and thus have the same continuum limit. The 4-fermion interaction we choose is of the Gross-Neveu, Nambu-Jona-Lasinio form [8,9]. Ideally, such an interaction should be chosen to have the $SU(N_f)\times SU(N_f)$ flavour symmetry of the original QCD action. However, we note that when one introduces auxiliary scalar and pseudoscalar fields to render this action quadratic in the fermion fields — which is necessary for lattice simulations, — the fermion determinant is no longer real, even in the continuum limit. Thus for 2 flavour QCD ($N_f = 2$), we make a simpler choice and choose a 4-fermion term with the symmetry $U(1) \times U(1) \subset SU(2) \times SU(2)$, where $U(1) \times U(1)$ is generated by $(\tau_3, \gamma_5\tau_3)$. The euclidean Lagrangian density for this theory is then

$$\mathcal{L} = \frac{1}{4}F_{\mu\nu}F_{\mu\nu} + \bar{\psi}(\not{D} + m)\psi - \frac{\lambda^2}{6N_f}[(\bar{\psi}\psi)^2 - (\bar{\psi}\gamma_5\tau_3\psi)^2]. \tag{1}$$

Lattice field theories incorporating fermions interacting both through gauge fields and through quartic self-interactions have been studied before — see for example [10]. Brower et al. [11] have suggested the addition of such chiral 4-fermion interactions to lattice QCD

[1]For the status of lattice QCD thermodynamics with the standard staggered action and two light flavours we refer the reader to recent publications [3,4]. Earlier work is summarised and referenced in recent reviews [5–7].

to control the singular nature of the zero mass Dirac operator. In addition, 4-fermion terms arise in systematic attempts to improve the fermion lattice action to make it better approximate the continuum action [12,13]. Our work was suggested by earlier work by one of us on lattice field theories with quartic 4-fermion actions [14–16] and by studies of the role such terms play in lattice QED.

We have simulated this theory using 2 flavours of staggered quarks on $8^3 \times 4$ and $12^2 \times 24 \times 4$ lattices, at an intermediate value of λ and zero quark mass, in order to determine the position and nature of the finite temperature transition. We also present some zero temperature results on an $8^3 \times 24$ lattice, where we demonstrate that the theory with massless quarks does indeed have a massless Goldstone pion. In addition to measuring the standard order parameters we have measured the pion, $\sigma(f_0)$, and a_0 screening masses to probe the nature of chiral symmetry restoration at this transition. We also simulated the corresponding theory with 4-fermion couplings but no gauge interactions on relatively small lattices (8^4 and $8^3 \times 4$) to aid us in deciding what values of 4-fermion coupling constant to choose.

In section 2 we discuss the lattice formulation of QCD with chiral 4-fermion interactions. We present our zero gauge-coupling results in section 3. The zero temperature results are given in section 4, while the finite temperature simulations and results are described in section 5. Section 6 gives discussions and conclusions, and outlines directions for future research.

II. LATTICE QCD WITH CHIRAL 4-FERMION INTERACTIONS

Equation 1 can be rendered quadratic in the fermion fields by the standard trick of introducing (non-dynamical) auxiliary fields σ and π in terms of which this Lagrangian density becomes

$$\mathcal{L} = \frac{1}{4} F_{\mu\nu} F_{\mu\nu} + \bar{\psi}(\not{D} + \sigma + i\pi\gamma_5\tau_3 + m)\psi + \frac{3N_f}{2\lambda^2}(\sigma^2 + \pi^2) \tag{2}$$

The molecular dynamics Lagrangian for a particular staggered fermion lattice transcription of this theory in which τ_3 is identified with ξ_5, the flavour equivalent of γ_5 is

$$L = -\beta \sum_{\Box} [1 - \frac{1}{3}\mathrm{Re}(\mathrm{Tr}_{\Box} UUUU)] + \frac{N_f}{8} \sum_s \dot{\psi}^\dagger A^\dagger A \dot{\psi} - \sum_{\tilde{s}} \frac{1}{8} N_f \gamma (\sigma^2 + \pi^2)$$
$$+ \frac{1}{2} \sum_l (\dot{\theta}_7^2 + \dot{\theta}_8^2 + \dot{\theta}_1^* \dot{\theta}_1 + \dot{\theta}_2^* \dot{\theta}_2 + \dot{\theta}_3^* \dot{\theta}_3) + \frac{1}{2} \sum_{\tilde{s}} (\dot{\sigma}^2 + \dot{\pi}^2) \quad (3)$$

where

$$A = \not{D} + m + \frac{1}{16} \sum_i (\sigma_i + i\epsilon\pi_i) \quad (4)$$

with i running over the 16 sites on the dual lattice neighbouring the site on the normal lattice, $\epsilon = (-1)^{x+y+z+t}$ and $\not{D}$ the usual gauge-covariant "d-slash" for the staggered quarks. The factor $\frac{N_f}{8}$ in front of the pseudo-fermion kinetic term is appropriate for the hybrid molecular dynamics algorithm with "noisy" fermions, where $A\dot{\psi}$ are chosen from a complex gaussian distribution with width 1. The "dots" represent derivatives with respect to molecular dynamics "time" as distinct from normal time. For the presentation of all our simulation results we use a time definition which is twice this, in order to be consistent with the convention used in the works of the HEMCGC and HTMCGC collaborations. We note that $\gamma = 3/\lambda^2$. Although the determinant of A does not appear to be real, it becomes so in the continuum limit. Without the gauge fields, this theory reverts to the one studied in [15], with $3N_f$ flavours.

The advantage of this choice of the chiral 4-fermion interaction is that it preserves the axial $U(1)$ chiral symmetry of the normal staggered quark lattice QCD action generated by $\gamma_5\xi_5$ at $m = 0$. This means that, when chiral symmetry is spontaneously broken, the pion associated with $\xi_5\gamma_5$ will be a true Goldstone boson and will be massless at $m = 0$, even for finite lattice spacing. Under this exact chiral symmetry the fields transform as

$$\dot{\psi}(n) \to e^{-i\frac{1}{2}\phi\epsilon(n)} \dot{\psi}(n) \quad (5)$$

$$\sigma(n) + i\pi(n) \to e^{i\phi} [\sigma(n) + i\pi(n)] \quad (6)$$

from which we find that

$$A\dot{\psi}(n) \to e^{i\frac{1}{2}\phi\epsilon(n)} A\dot{\psi}(n) \tag{7}$$

$$\sigma(n) + i\epsilon(n)\pi(n) \to e^{i\phi\epsilon(n)}[\sigma(n) + i\epsilon(n)\pi(n)], \tag{8}$$

when $m = 0$. Hence, for massless quarks the above Lagrangian has an exact $U(1)$ flavour axial symmetry.

III. THE NAMBU-JONA-LASINIO-GROSS-NEVEU MODEL.

In order to ascertain which ranges of values of γ represent strong coupling and which represent weak coupling, we simulated the above lattice theory without the gluon fields where it becomes the lattice version of the Nambu-Jona-Lasinio-Gross-Neveu model with $3N_f = 6$ flavours [9,8,15]. We have simulated this theory with $m = 0$ on 8^4 and $8^3 \times 4$ lattices. For these simulations, we ran for 5000 molecular-dynamics time units at each γ value with step size $dt = 0.05$.

This theory is known to have a phase transition, even at zero temperature, as a function of γ [17]. For strong coupling (small γ) chiral symmetry is spontaneously broken, while at weak coupling (large γ) chiral symmetry remains unbroken. Since the theory is strictly massless, the direction this axial symmetry is broken is arbitrary, and the chiral condensate is a linear combination of $\langle\bar{\psi}\psi\rangle$ and $i\langle\bar{\psi}\gamma_5\xi_5\psi\rangle$ (or σ and π). Because we work on finite lattices, the direction of this symmetry breaking does not remain constant, but rotates over the course of the run. For this reason, the order parameter we will denote by $\langle\bar{\psi}\psi\rangle$ is actually the molecular-dynamics time average of $\sqrt{\langle\bar{\psi}\psi\rangle^2 - \langle\bar{\psi}\gamma_5\xi_5\psi\rangle^2}$, which differs from the true chiral condensate by terms $\mathcal{O}(1/\sqrt{V})$ where V is the space-time volume of the lattice. This quantity is given in figure 1 as a function of γ for both lattice sizes.

From the 8^4 lattice we conclude that the zero temperature phase transition from the strong coupling phase to the weak coupling phase occurs somewhere in the range $1.7 \lesssim$

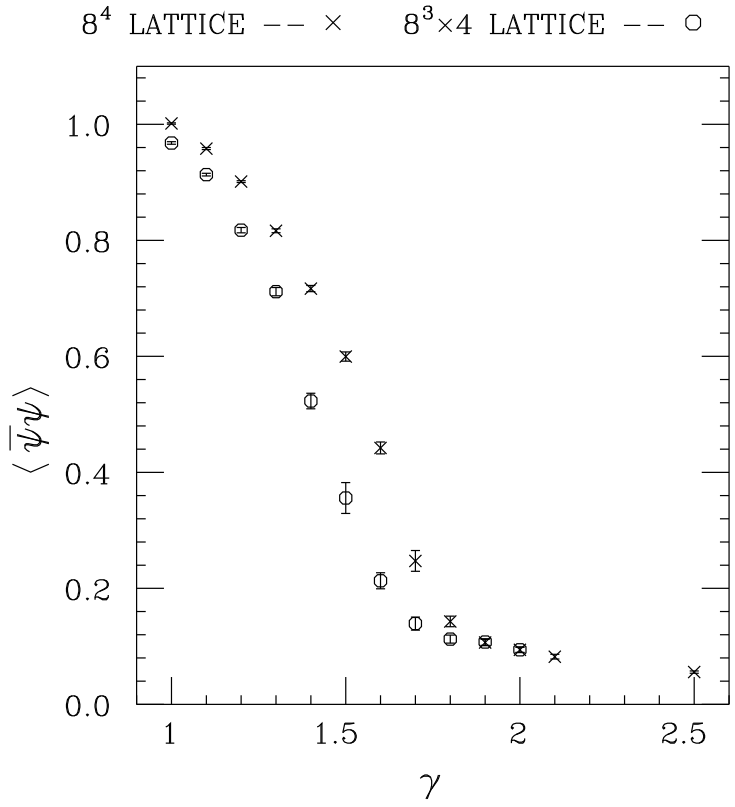

FIG. 1. $\langle\bar{\psi}\psi\rangle$ as a function of γ for the pure 4-fermion theory for both zero and finite temperatures.

$\gamma \lesssim 1.8$, while the finite temperature transition on the 8^3 lattice occurs at a somewhat smaller value of γ. Thus we would conclude that since, for lattice QCD with chiral 4-fermion interactions, we wish to work in the weak 4-fermion coupling regime, we should restrict ourselves to values of γ which are greater than 2. Moreover, since the introduction of this 4-fermion term produces chiral phase transitions where none previously existed, we could expect that chiral symmetry might be restored at a temperature higher than the deconfinement temperature. Since this is not the case for normal lattice QCD, we should try to work at a large enough γ value that the 2 transitions are close, if not coincident. We describe studies to determine the appropriate range of γ values in section 5.

IV. ZERO TEMPERATURE RESULTS

We have undertaken a preliminary investigation of the hadron spectrum of QCD with chiral 4-fermion interactions of the type discussed in section 2 on an $8^3 \times 24$ lattice with 2 flavours of massless quarks at $\beta = 6/g^2 = 5.4$ and $\gamma = 10$. $\beta = 5.4$ was chosen since it lies just below the phase transition for lattice QCD without the 4-fermion term on an $N_t = 8$ lattice. Thus we were assured of being in the confined phase. We used the hybrid molecular dynamics method with time increment $dt = 0.05$ for updating. We ran for a total of 5000 time units, discarding the first 1000 time units for equilibration. 250 configurations spaced by 20 time units were saved for further analysis. The first 50 of these were discarded for equilibration.

The pion and σ propagators were calculated from the correlations of the π and σ fields, sampled every 2 time units. Because, as was the case in the previous section, the direction of chiral symmetry breaking rotates during a run on a finite lattice, we chirally rotated each (σ, π) configuration (see equation 6) so that $\sum_{sites} \pi = 0$. The propagators are then given by

$$P_\sigma(T) = \frac{1}{V} \sum_t \langle \sum_{\mathbf{x}} \sigma(\mathbf{x}, t) \sum_{\mathbf{y}} \sigma(\mathbf{y}, t+T) \rangle - v \langle \sigma \rangle^2 \tag{9}$$

$$P_\pi(T) = \frac{1}{V} \sum_t \langle \sum_{\mathbf{x}} \pi(\mathbf{x}, t) \sum_{\mathbf{y}} \pi(\mathbf{y}, t+T) \rangle \tag{10}$$

where V is the space-time and v is the spatial volume of the lattice. Correlated fits are made to these propagators, binning over 10 measurements (20 time units) to account for correlations, and using jackknife to remove the vacuum expectation values in the σ propagator.

The π propagator was fitted to the form

$$P_\pi(T) = A P_0(T) - B \tag{11}$$

where $P_0(T)$ is the lattice propagator for a massless scalar boson

$$P_0(T) = \frac{1}{2N_t} \sum_{k=-N_t/2+1}^{N_t/2} \frac{e^{2\pi i k T/N_t}}{(1 - cos(2\pi k/N_t)}, \tag{12}$$

with the $k = 0$ mode excluded. We found $A = 3.7(1)$ and $B = 7.5(1)$ for the fit from $T = 1$ to $T = 12$. This fit has a 78% confidence level. Figure 2 shows the measured propagator with this fit superimposed. As indicated by the high confidence level, our measured pion propagator is very well fit by a massless scalar propagator, except at $T = 0$ where we see the remnant of the original δ-function interaction. Thus the sum of fermion "bubble" diagrams has converted the auxilliary π field to a true Goldstone pion.

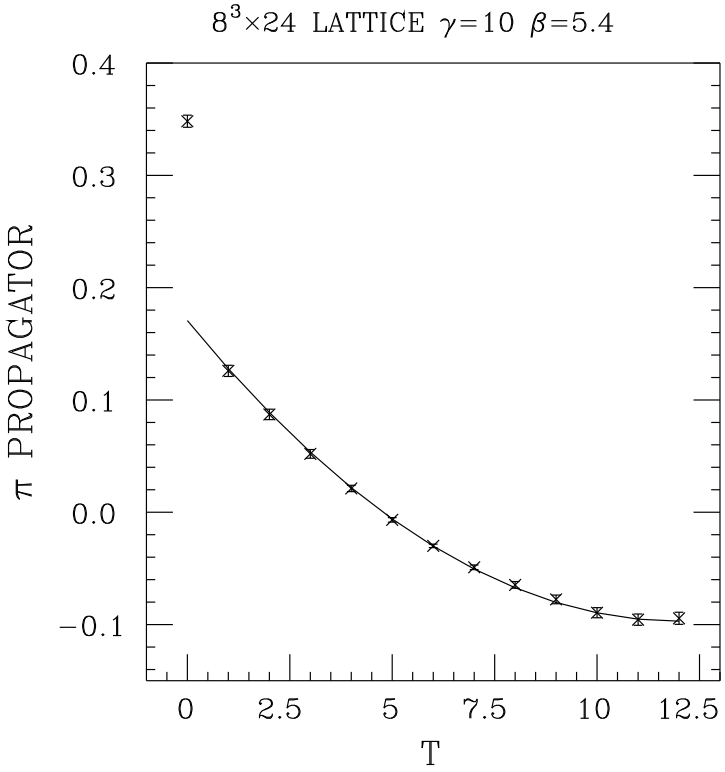

FIG. 2. The π propagator at zero temperature, the curve is a fit to a massless scalar boson.

For large T the sigma propagator should behave as

$$P_\sigma(T) = A[e^{-m_\sigma T} + e^{-m_\sigma(N_t-T)}] + B[e^{-m_{\pi_2} T} + e^{-m_{\pi_2}(N_t-T)}] \tag{13}$$

We have attempted such fits, but are unable to find a stable value for the π_2 mass. For this reason we resorted to the single particle fit obtained by setting B to zero. Here, our best fit yielded $m_\sigma = 1.16(24)$ with a 51% confidence level. This mass was consistent with those obtained from the 2 particle fits. We have plotted our σ propagator and this fit in

figure 3. Here it is clear why our fits were so poor — the propagator disolves into noise after only a few time-slices, which is the usual problem encountered when trying to calculate high mass propagators as in equation 9. (Here the error in the propagator is expected to be independent of T, whereas for meson propagators calculated directly from the quark propagator, the error falls with increasing T). It is interesting to speculate as to whether the "tail" of this propagator is due to the 2-pion cut in the σ propagator.

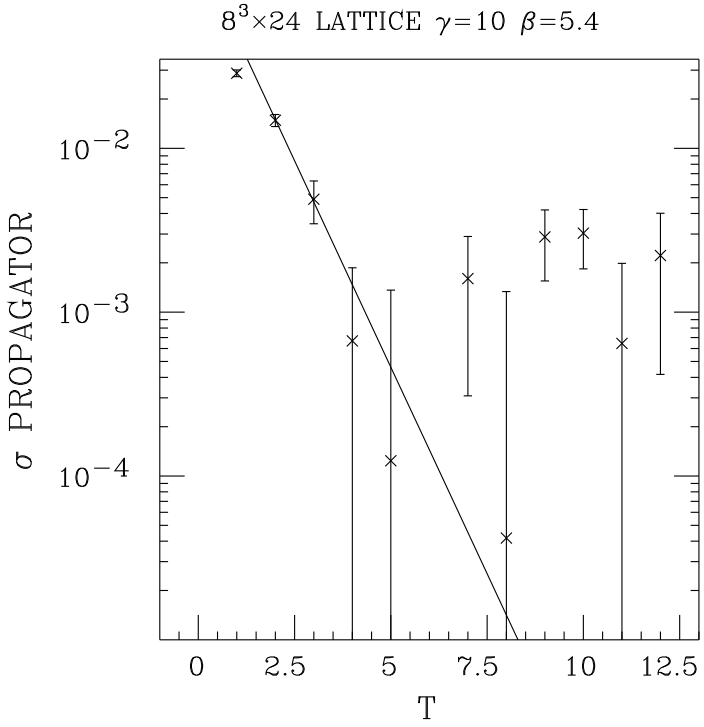

FIG. 3. The σ propagator at zero temperature, the curve is the single particle fit described in the text.

V. FINITE TEMPERATURE RESULTS

We have performed simulations on $N_t = 4$ lattices and with 2 flavours of zero mass quarks, in order to study the transition from hadronic matter to a quark gluon plasma at finite temperature. Our initial runs were performed on $8^3 \times 4$ lattices with $\gamma = 2.5$, 5, and 10 The time step $dt = 0.05$ for these runs. We experimented with values of dt from 0.02 to 0.20, and found $dt = 0.05$ to be small enough that finite dt errors were smaller

than statistical errors. We measured the Wilson/Polyakov line and the chiral condensate, $\langle\bar{\psi}\psi\rangle$, enabling us to determine the phase structure of the theory. Since, as we have seen in section 3, the presence of the 4-fermion coupling can break chiral symmetry, even at zero gauge coupling where there is no confinement, we expect that the chiral symmetry restoration and deconfinement will in general occur at different values of β. In fact for values of γ less than that for the transition at zero gauge coupling, chiral symmetry will always be broken. In figure 4 we show the values of the 2 order parameters for each of $\gamma = 2.5$, 5, and 10. It is clear at $\gamma = 2.5$ that the deconfinement transition, marked by the rapid increase in the Wilson/Polyakov line (around $\beta = 5$), occurs at a much lower value of β than the chiral symmetry restoration, marked by a drop in $\langle\bar{\psi}\psi\rangle$ (which does not reach zero for the reasons given in section 3) between $\beta = 6$ and 10. At $\gamma = 5$ the 2 transitions still appear to be distinct, although we cannot rule out this being a finite volume effect, while at $\gamma = 10$ the 2 transitions appear to be coincident. Since we are interested in obtaining results which are relevant to the continuum limit where the 4-fermion coupling vanishes and the 2 transitions *are* believed to be coincident, we chose to work at $\gamma = 10$.

At $\gamma = 10$, we observed signs of a two state signal in the time evolution of both order parameters at $\beta = 5.33$, indicating the possibility of a first order transition. Figure 5 shows the time evolution of the Wilson/Polyakov line at this β value. Thus we conclude that the transition occurs at $\beta = 5.330(5)$ on this size lattice. Since the standard action shows a false first order transition on small lattices, we repeated our runs on a $12^2 \times 24 \times 4$ lattice. Having $N_z = 24$ enabled us to measure hadronic screening lengths in the z direction. On this larger lattice, we find evidence for 2-state signals at $\beta = 5.325$ and $\beta = 5.33$. In figure 6 we show the time evolution of the Wilson/Polyakov line for these 2 β values. At $\beta = 5.325$ the Wilson line measured from a cold start remains small for the total length of the run while that from a hot start, remains large for over 3000 time units before it tunnels rapidly to a low value and stays there. At $\beta = 5.33$ the Wilson line from a hot start remains high for the entire run, while that from a cold start remains low for over 1500 time units before it tunnels

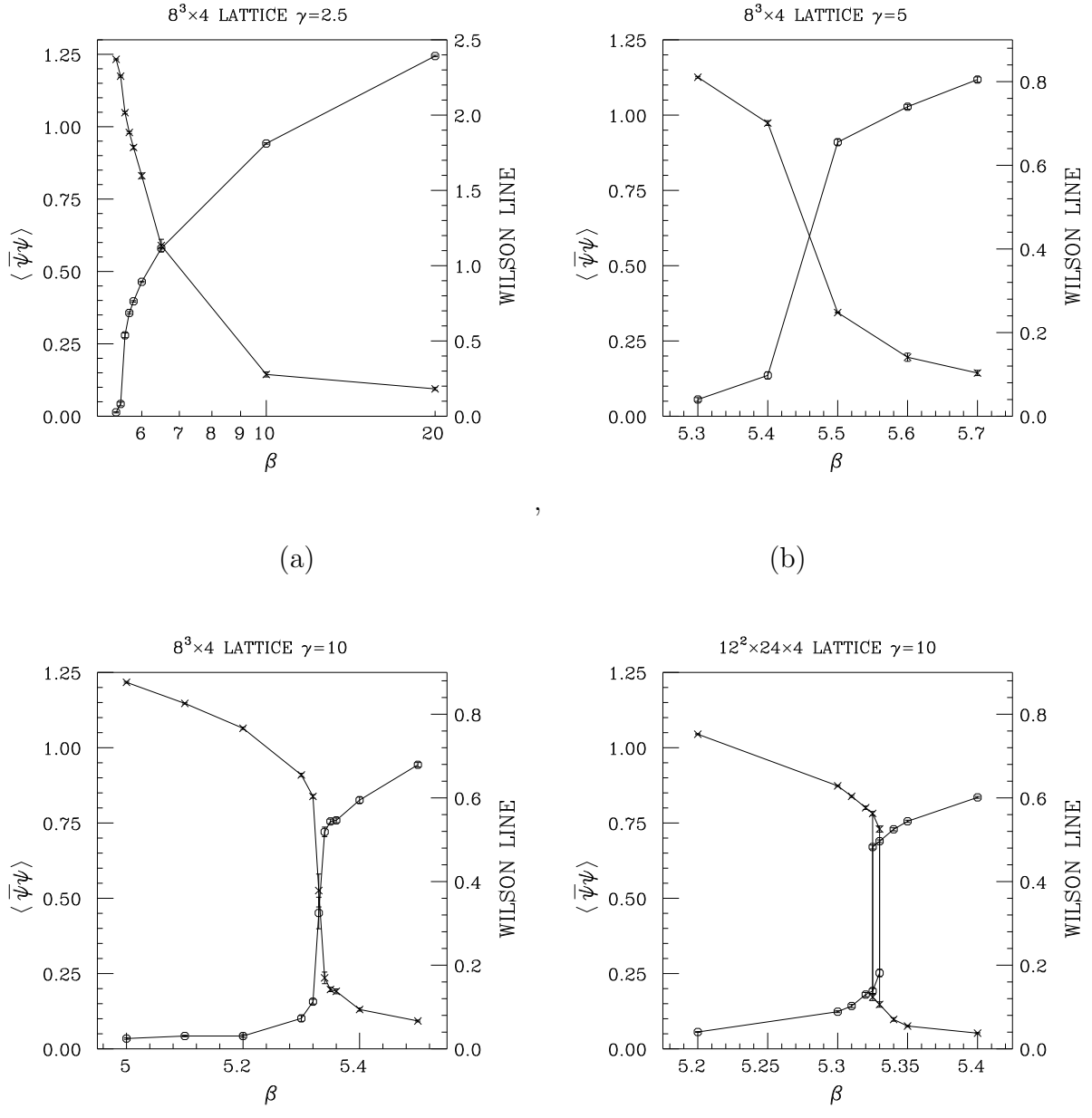

FIG. 4. Wilson/Polyakov line (circles) and $\langle\bar{\psi}\psi\rangle$ (crosses) versus β for a) An $8^3 \times 4$ lattice at $\gamma = 2.5$, b) An $8^3 \times 4$ lattice at $\gamma = 5$, c) An $8^3 \times 4$ lattice at $\gamma = 10$, and d) A $12^2 \times 24 \times 4$ lattice at $\gamma = 10$.

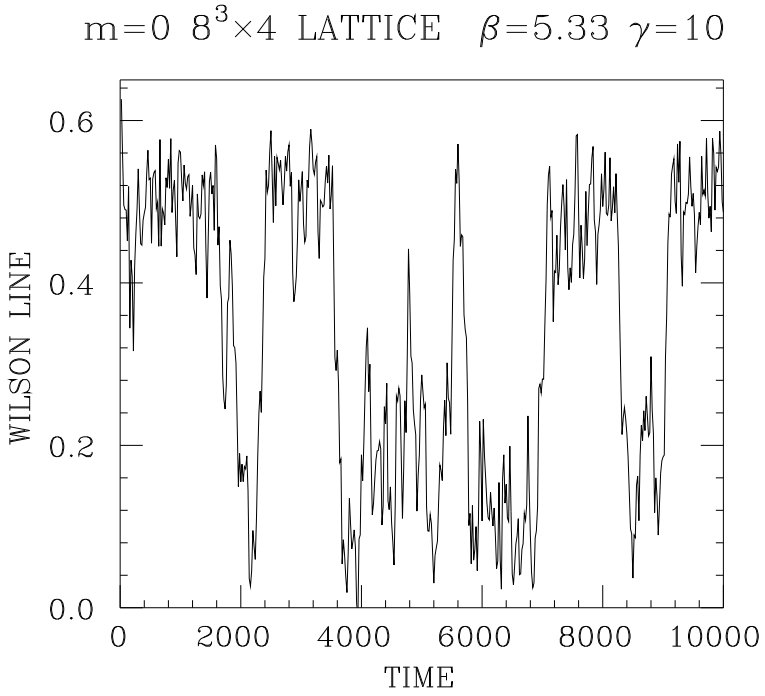

FIG. 5. The time evolution of the Wilson/Polyakov line at $\beta = 5.33$ on an $8^3 \times 4$ lattice.

rapidly to a high value and stays there. There is no sign of metastability for higher or lower β values. We thus conclude that the transition occurs in the range $5.325 \lesssim \beta \lesssim 5.33$, and probably closer to $\beta = 5.325$. The values of these quantities, $\langle\sigma\rangle$ and the average plaquette, $\langle 1 - \frac{1}{3}\mathrm{Tr}U_\Box\rangle$ are given in tables I,II. We note that the required relationship

$$\langle\bar{\psi}\psi\rangle = \gamma\langle\sigma\rangle \tag{14}$$

is approximately true in the chirally broken phase, but that in the chirally symmetric phase it is somewhat less well obeyed. Since the continuum values of both these quantities are zero in this symmetric phase, this suggests that the difference is in the $\sqrt{1/V}$ departures of our estimators for these quantities from their true values, which do not have to obey this relationship.

We now turn to a consideration of the hadronic screening lengths which measure the propagation of exitations with hadronic quantum numbers in hadronic matter and the quark-gluon plasma. In particular these measure the manner in which chiral symmetry is

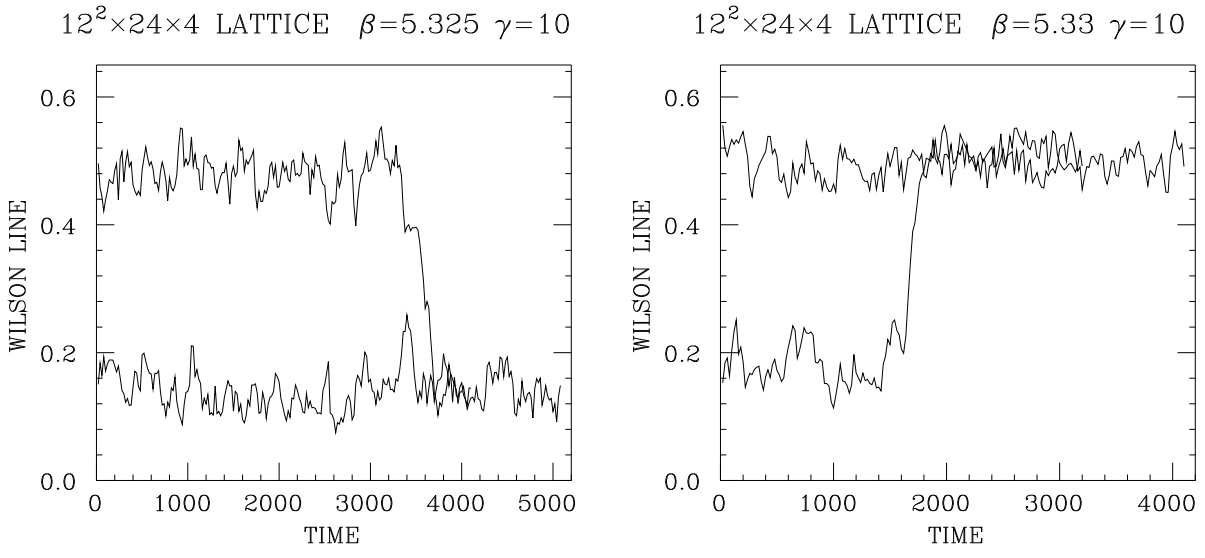

(a) (b)

FIG. 6. Time evolution of the Wilson/Polyakov line on a $12^3 \times 24 \times 4$ lattice a) at $\beta = 5.325$ and b) at $beta = 5.33$.

restored as we pass through the transition from hadronic matter to a quark-gluon plasma. Here we concentrate on the π and $\sigma(f_0)$ propagators which can be calculated from the π and σ auxiliary fields, as in section 2, i.e. from

$$P_\sigma(Z) = \frac{1}{V}\sum_z \langle \sum_{xyt} \sigma(x,y,z,t) \sum_{x'y't'} \sigma(x',y',z+Z,t') \rangle - N_x N_y N_t \langle\sigma\rangle^2 \tag{15}$$

$$P_\pi(Z) = \frac{1}{V}\sum_z \langle \sum_{xyt} \pi(x,y,z,t) \sum_{x'y't'} \pi(x',y',z+Z,t') \rangle \tag{16}$$

In the hadronic phase we fit the pion propagator to

$$P_\pi(Z) = AP_0(Z) - B \tag{17}$$

where $P_0(Z)$ is the lattice propagator for a massless scalar boson

$$P_0(Z) = \frac{1}{2N_z} \sum_{k=-N_z/2+1}^{N_z/2} \frac{e^{2\pi i k Z/N_z}}{(1 - cos(2\pi k/N_z)} \tag{18}$$

with the $k = 0$ mode excluded. The σ propagator was fitted to

$$P_\sigma(Z) = A[e^{-m_\sigma Z} + e^{-m_\sigma (N_z - Z)}] + B[e^{-m_{\pi_2} Z} + e^{-m_{\pi_2}(N_z - Z)}] \tag{19}$$

β	time	Wilson Line	$\langle\bar{\psi}\psi\rangle$	$\langle\sigma\rangle$	PLAQUETTE
5.0	2000	0.025(2)	1.217(3)	0.1235(5)	0.5825(3)
5.1	2000	0.031(2)	1.147(2)	0.1170(5)	0.5636(3)
5.2	1000	0.031(4)	1.065(4)	0.1080(7)	0.5430(8)
5.3	1000	0.073(7)	0.910(5)	0.0923(8)	0.5149(7)
5.32	6000	0.113(6)	0.838(6)	0.0857(8)	0.5064(6)
5.33	10000	0.325(38)	0.526(55)	0.0575(48)	0.4900(24)
5.34	4000	0.519(11)	0.236(19)	0.0290(17)	0.4746(5)
5.35	2000	0.544(5)	0.197(7)	0.0260(8)	0.4717(4)
5.36	2000	0.546(6)	0.191(8)	0.0254(9)	0.4699(4)
5.4	1000	0.595(7)	0.131(5)	0.0203(8)	0.4619(4)
5.5	1000	0.679(5)	0.093(3)	0.0173(6)	0.4469(3)

TABLE I. Wilson line, $\langle\bar{\psi}\psi\rangle$, $\langle\sigma\rangle$ and average plaquette as functions of β for an $8^3 \times 4$ lattice at $\gamma = 10$. The "time" is the molecular dynamics time for the run. Typically 1/5 of each run was discarded for equilibration.

and to the special case where $B = 0$, which was often adequate in this range of β values. Above the transition, in the quark-gluon plasma phase, since $\langle\bar{\psi}\psi\rangle = \gamma\langle\sigma\rangle = 0$, one cannot distinguish σ and π and it makes most sense to consider

$$P_{\sigma\pi} \equiv P_\sigma + P_\pi, \tag{20}$$

which we fit to

$$P_{\sigma\pi}(Z) = A[e^{-m_{\sigma\pi}Z} + e^{-m_{\sigma\pi}(N_z - Z)}] \tag{21}$$

Since choosing to fit our pion to a massless scalar boson propagator below the transition, and to a massive propagator above might seem to be forcing the result we want, we have looked at fits to the pion propagator obtained as in section 2 by chirally rotating our propagators so that $\langle\pi\rangle = 0$, and then fitting to 17. The results obtained from our best

β	time	Wilson Line	$\langle\bar{\psi}\psi\rangle$	$\langle\sigma\rangle$	PLAQUETTE
5.2	2140	0.040(1)	1.045(2)	0.1056(3)	0.5427(2)
5.3	2040	0.089(20	0.873(2)	0.0887(3)	0.5136(3)
5.31	2080	0.103(4)	0.838(4)	0.0849(5)	0.5096(3)
5.32	4020	0.130(5)	0.801(6)	0.0809(5)	0.5055(4)
5.325c	4100	0.138(6)	0.782(6)	0.0794(6)	0.5034(4)
5.325h	5080	0.483(5)	0.172(11)	0.0184(12)	0.4790(3)
5.33c	3200	0.181(9)	0.730(10)	0.0742(9)	0.4994(6)
5.33h	4100	0.496(3)	0.147(9)	0.0163(9)	0.4775(2)
5.34	2080	0.525(4)	0.098(6)	0.0116(6)	0.4743(2)
5.35	2080	0.544(3)	0.076(2)	0.0096(3)	0.4716(1)
5.4	2020	0.601(2)	0.052(2)	0.0079(3)	0.4621(1)

TABLE II. Wilson line, $\langle\bar{\psi}\psi\rangle$, $\langle\sigma\rangle$ and average plaquette as functions of β for an $12^2 \times 24 \times 4$ lattice at $\gamma = 10$. The "time" is the molecular dynamics time for the run. Typically 1/5 of each run was discarded for equilibration. h and c refer to runs from hot and cold starts. Where a tunneling occurs, we only average over pretunneling data.

fits are given in table III. As in the zero temperature case we bin our data in bins of 10, i.e. 20 time units. Note that, for all our mass fits we have selected our runs from a cold start for $\beta = 5.325$ and from a hot start for $\beta = 5.33$, which folds in our knowledge that the transition occurs in the range $5.325 < \beta < 5.33$ We note that the coefficient A which measures the amount of massless scalar propagator in this fit drops abruptly as we increase β through the phase transition, and continues to drop as β is increased. In addition, the parameters of the fits become more sensitive to the fitting range as β is increased beyond this transition. Thus we feel justified in taking the pion screening mass to be zero below the transition, as required by Goldstone's theorem, while fitting it to a massive propagator above the transition.

β	range	A	B	confidence
5.2	1 – 11	0.0051(2)	0.0069(2)	0.832
5.3	2 – 12	0.0044(3)	0.0079(4)	0.639
5.31	1 – 12	0.0045(2)	0.0072(2)	0.739
5.32	1 – 11	0.0042(1)	0.0075(1)	0.248
5.325	1 – 11	0.0047(2)	0.0069(1)	0.858
5.33	2 – 5	0.0028(1)	0.0133(18)	0.739
5.34	2 – 12	0.0020(1)	0.0101(4)	0.475
5.35	4 – 10	0.0010(1)	0.0164(12)	0.642
5.4	3 – 8	0.0006(1)	0.0155(8)	0.567
5.5	3 – 12	0.00009(6)	-0.0035(12)	0.528

TABLE III. Coefficients A and B for the fit of the pion propagator to a massless scalar boson (equation 17).

Above the transition, our definition of $\langle\bar{\psi}\psi\rangle$ should not vanish, but rather should scale as $1/\sqrt{v}$, and so vanish in the in the infinite (spatial) volume limit. In table IV we compare $\langle\bar{\psi}\psi\rangle$ measured on the $12^2 \times 24 \times 4$ with $\sqrt{8^3/(12^2 \times 24)} \times \langle\bar{\psi}\psi\rangle$, measured on the $8^3 \times 4$ lattice, and the corresponding values of $\langle\sigma\rangle$ for values of β above the transition,

β	$\langle\bar{\psi}\psi\rangle_{12^2\times24\times4}$	$\sqrt{4/27} \times \langle\bar{\psi}\psi\rangle_{8^3\times4}$	$\langle\sigma\rangle_{12^2\times24\times4}$	$\sqrt{4/27} \times \langle\sigma\rangle_{8^3\times4}$
5.33	0.147(9)	0.202(21)	0.0163(9)	0.0221(18)
5.34	0.098(6)	0.091(7)	0.0116(6)	0.0111(7)
5.35	0.076(2)	0.076(3)	0.0096(3)	0.0100(3)
5.4	0.052(2)	0.050(2)	0.0079(3)	0.0078(3)

TABLE IV. Test of $\langle\bar{\psi}\psi\rangle$ scaling in the high temperature phase.

Except for $\beta = 5.33$ which really should not have been included, since the $8^3 \times 4$ data really represents a mixture of high and low temperature phases, scaling is true within our statistical errors. This helps justify our conclusion that chiral symmetry is indeed restored

in the high temperature phase, and our choice of screening propagator fits based on this assumption. The fact that this scaling is true for both quantities is an indication that the departures from the relationship between them is an artifact of the $\sqrt{1/v}$ difference between these quantities and the vacuum condensates they represent, as suggested above.

Our σ and π screening mass fits are shown in figure 7. Below the transition the σ mass falls steeply as the transition is approached. What is unclear is whether it actually falls to zero at the transition. The pion is massless in this regime. Above the transition the σ/π mass rises rapidly from a small and possibly zero value at the transition, and is expected to approach $2\pi T = 2\pi/N_t = \pi/2$ as $\beta \to \infty$. Thus the restoration of the $U(1) \times U(1) \subset SU(2) \times SU(2)$ chiral symmetry is manifest in the spectrum of screening masses/screening lengths.

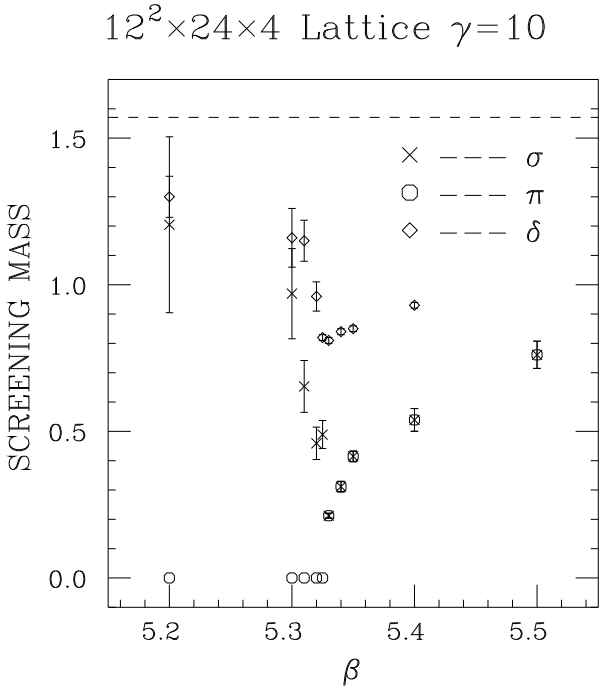

FIG. 7. The $\sigma(f_0)$ and π screening masses as functions of β.

In addition to the π and σ, figure 7 shows the screening masses in the flavor triplet scalar channel, $\delta(a_0)$. These are obtained from measurements of the "connected" part of

the σ propagator (i.e. one quark "bubble" instead of the complete "chain of bubbles"). In contrast with the σ and π, the δ always remains heavy. We therefore have a situation where the $U_A(1)$ axial symmetry only becomes effectively restored at temperatures well above the chiral phase transition, in agreement with [19,20]. The splitting between δ and σ or π is very clear in this study because we work at zero quark mass [2] The screening mass of the δ also exhibits a jump (or rapid crossover) which is consistent with our determination of a first order transition.

Finally we have measured observables associated with the entropy density, energy density and pressure. We present these as is, since tree level extractions of entropy density, energy density and pressure are unphysical (they require $p = \frac{1}{3}\epsilon$, the ideal gas relation, which cannot hold through a first order transition where pressure is continuous and energy density is discontinuous), and the one loop calculations have yet to be calculated. In addition, for the energy density and pressure, we need zero temperature measurements of observables at the same β values. The 3 observables given in table V are related to the contributions of the gauge fields, the quark fields and the chiral 4-fermion interactions respectively, to the entropy density. What is most noticable is that each of these quantities shows a sizable jump at the transition indicating that there will indeed be a significant increase in entropy across this transition. This helps substantiate our conclusion that the transition is first order. On the other hand, the variation of each of these quantities on either side of this transition is modest.

---

[2]Simulations closer to the continuum limit will however be necessary in order to make sure that this splitting is not induced by spurious symmetry breakings at moderate values of β and γ.

β	$\beta(P_{st} - P_{ss})$	$\langle\bar{\psi}\not{D}_0\psi\rangle - \frac{3}{4}$	$\frac{1}{8}N_f\gamma(\sigma^2 + \pi^2)$
5.2	0.0001(13)	-0.0298(5)	1.0362(4)
5.3	0.0067(10)	-0.0145(6)	1.0282(4)
5.31	0.0081(11)	-0.0125(8)	1.0264(4)
5.32	0.0105(8)	-0.0070(10)	1.0259(3)
5.325	0.0116(8)	-0.0049(11)	1.0250(3)
5.33	0.0563(7)	0.0632(6)	1.0118(2)
5.34	0.0587(6)	0.0672(6)	1.0109(4)
5.35	0.0599(7)	0.0692(5)	1.0104(4)
5.4	0.0605(9)	0.0716(4)	1.0094(3)
5.5	0.0588(9)	0.0738(3)	1.0087(3)

TABLE V. Observables relevant to entropy density, energy density and pressure as functions of β.

VI. SUMMARY AND CONCLUSIONS

The action for lattice QCD with 2 flavours of staggered quarks is modified by the addition of a chiral 4-fermion interaction. The chosen 4-fermion interaction has a $U(1) \times U(1) \subset SU(2) \times SU(2)$ symmetry, where $SU(2) \times SU(2)$ is the normal $SU(N_f) \times SU(N_f)$ chiral flavour symmetry of QCD with massless quarks. This irrelevant interaction alows us to simulate at zero quark mass by rendering the Dirac operator non-singular.

We have performed simulations at $\gamma = 3/\lambda^2 = 10$, a relatively weak value for the 4-fermion coupling, and zero quark mass at both zero and finite temperatures. The zero temperature calculation was performed on an $8^3 \times 24$ lattice at $\beta = 6/g^2 = 5.4$, and was meant as a precurser to performing serious hadron spectroscopy with this action. Our major result was clear evidence of a massless Goldstone pion, the other hadrons having relatively large masses (in lattice units) for gauge couplings and hence lattice spacings this large. The effectiveness of the 4-fermion term in rendering the Dirac operator non-singular is reflected

in that the average number of conjugate gradient iterations required to invert the Dirac operator was < 250.

The finite temperature simulations were performed on $12^2 \times 24 \times 4$ and $8^3 \times 4$ lattices. The finite temperature transition occured at $\beta_c = 5.327(2)$, which is to be compared with $\beta_c = 5.225(5)$, estimated for the massless quark extrapolation with the standard action [7]. We have seen clear evidence that the transition is a strong first order transition. Since we believe that the actual continuum transition should be second order (or possibly weakly first order) [18] which is what simulations with the standard action suggest [3–7], we believe this to be due to the size of the 4-fermion interaction, enhanced by the strength of the gauge coupling. Again the condition of the Dirac operator was well under control, it requiring < 400 conjugate gradient iterations, on average, to invert this operator throughout the range of β's considered. We are now running at $N_t = 4$ with $\gamma = 20$, and $N_t = 6$ with $\gamma = 10$ and $\gamma = 20$. Preliminary results at $N_t = 6$ suggest a second order transition at $\gamma = 10$, which is even clearer at $\gamma = 20$. It is still too early to draw any conclusions from the ongoing runs at $N_t = 4$, $\gamma = 20$. The π and σ screening masses showed the appropriate behaviour. The Goldstone pion mass remained zero below the transition, and increased from zero after the transition. The σ mass dipped as the transition was approached from below (it is not clear whether it actually approached zero on the cold side of the transition), and rose, apparently from zero, above the transition where it was degenerate with the pion mass. The other screening masses remained large across the transition. In particular the connected part of the σ propagator, the $\delta(a_0)$ ramained large over this region. However, flavour symmetry violation is large enough at these β and γ values that it is not clear whether this is further evidence that the flavour singlet $U(1)_A$ symmetry remains broken across the transition from hadronic matter to a quark-gluon plasma [19,20].

If our thermodynamics simulations at larger N_t and/or γ do indicate a second order transition, we should be able to determine the universality class of this transition and the critical indices, enabling us to determine the equation of state of hadronic matter. With still

larger N_t we should be able to measure asymptotic scaling and determine the position, as well as nature of the phase transition. At zero temperature we should be able to obtain the hadronic spectrum, first at zero mass and then at the physical quark masses *without* having to perform an extrapolation in quark mass.

We are investigating how one might overcome the difficulties with simulating with a 4-fermion term having the more physical $SU(2) \times SU(2)$ chiral symmetry, and perhaps $U(2) \times U(2)$ chiral symmetry. In addition we will investigate combining this improvement to the standard lattice QCD action with the improvements of Lepage *et al.* [21], or of the "perfect action" methods [22].

Preliminary results of these simulations were reported at LATTICE'97 [23].

VII. ACKNOWLEDGEMENTS

These computations were performed on the CRAY C-90 at NERSC. This work was supported by the U. S. Department of Energy under contract W-31-109-ENG-38, and the National Science Foundation under grant NSF-PHY92-00148. We would like to thank John Sloan and Misha Stephanov for informative conversations.

REFERENCES

[1] F. Karsch and E. Laermann, Phys. Rev. D **50**, 6954 (1994).

[2] T. Blum *et al.*, Phys. Rev. D **51**, 5153 (1995); C. Bernard *et al.*, Phys. Rev. D **55**, 6861 (1997).

[3] C. Bernard *et al.*, Phys. Rev. D **54**, 4585 (1996).

[4] S. Gottlieb et al., Phys. Rev. D **55**, 6852 (1997).

[5] A. Ukawa, Nucl. Phys. B(Proc. Suppl.) **53**, 106 (1997).

[6] K. Kanaya, Nucl. Phys. B(Proc. Suppl.) **47**, 144 (1996).

[7] F. Karsch, Nucl. Phys. B(Proc. Suppl.) **34**, 63 (1994).

[8] D. J. Gross and A. Neveu, Phys. Rev. D **20**, 3235 (1974).

[9] Y. Nambu and G. Jona-Lasinio, Phys. Rev. **122**, 345 (1961).

[10] K. I. Kondo, H. Mino and K. Yamawaki, Phys. Rev. D **39**,2430 (1989).

[11] R. C. Brower, Y. Shen and C.-I. Tan, Boston University preprint BUHEP-94-3 (1994); R. C. Brower, K. Orginos and C.-I. Tan, Nucl. Phys. B(Proc. Suppl.) **42** (1995).

[12] B. Sheikholeslami and R. Wohlert, Nucl. Phys. **B259**, 572 (1985).

[13] T. Blum *et al.*, Phys. Rev. D **55**, R1133 (1997).

[14] S. Hands, A. Kocic and J. B. Kogut, Ann. Phys. **224** (1993).

[15] S. Kim, A. Kocic and J. B. Kogut, Nucl. Phys. **B429**, 407 (1994).

[16] S. Hands and J. B. Kogut, e-print hep-lat/9705038 (1997).

[17] S. Hands, S. Kim and J. B. Kogut, Nucl. Phys. **B442**, 364 (1995).

[18] R. Pisarski and F. Wilczek, Phys. Rev. D **29**, 338 (1984).

[19] J. B. Kogut, J.-F. Lagae and D. K. Sinclair, Nucl. Phys. B(Proc. Suppl.) **53**, 269 (1997).

[20] C. Bernard *et al.*, Nucl. Phys. B(Proc. Suppl.) **53**, 442 (1997).

[21] M. Alford *et al.*, Phys. Lett. **B361**, 87 (1995).

[22] P. Hasenfratz and F. Niedermayer, Nucl. Phys. **B414** (1994).

[23] J. B. Kogut and D. K. Sinclair, Nucl. Phys. B(Proc. Suppl.) **53**, 272 (1997).